TiOxNy coatings grown by atmospheric pressure metal organic chemical vapor deposition

Francis Maury, Florin-Daniel Duminica

TiO_xN_y coatings grown by atmospheric pressure metal organic chemical vapor deposition

F. Maury *, F.-D. Duminica

CIRIMAT, CNRS/INPT/UPS, ENSIACET, 4 allée E. Monso, BP 44362, 31030 Toulouse cedex 4, France

Keywords:
Atmospheric pressure CVD
MOCVD
TiO_xN_y
Hard coatings

A B S T R A C T

Titanium oxynitride coatings were deposited on various substrates by an original atmospheric pressure metal organic chemical vapor deposition (MOCVD) process using titanium tetra-*iso*-propoxide as titanium and oxygen precursors and hydrazine as a nitrogen source. The films composition was monitored by controlling the N_2H_4 mole fraction in the initial reactive gas phase. The variation of the N content in the films results in significant changes in morphological, structural and mechanical properties. When a large excess of the nitrogen source is used the resulting film contains *ca* 17 at % of nitrogen and forms dense and amorphous TiO_xN_y films. Growth rates of these amorphous $TiO_{1.5}N_{0.5}$ coatings as high as 14 μm/h were obtained under atmospheric pressure. The influence of the deposition conditions on the morphology, the structure, the composition and the growth rate of the films is presented. For the particular conditions leading to the growth of amorphous $TiO_{1.5}N_{0.5}$ coatings, first studies on the mechanical properties of samples grown on stainless steel have revealed a high hardness, a low friction coefficient, and a good wear resistance in unlubricated sliding experiments against alumina which make them very attractive as protective metallurgical coatings.

1. Introduction

Coatings in the ternary system Ti-O-N have many technological applications due to their electrical, optical and mechanical properties and their good thermal stability. For instance TiO_2 exhibits a high dielectric constant and electrical resistivity, a high refractive index and a good optical transparency over a wide spectral range. Furthermore anatase is well known as a large band gap semiconductor for its photocatalytic activity under UV irradiation. On the other hand, titanium nitride has a good thermal and electrical conductivity and a high hardness. TiN is widely used as a metallurgical coating for instance in cutting tools as a wear-resistant coating and as a diffusion barrier in large scale integrated circuits. There is also an increasing attention for titanium oxynitride coatings due to their interesting physical properties that lead to applications in optically selective absorbing films to enhance the contrast of cathode-ray tube displays [1], such as antireflection coatings [2], electrically switchable windows [3], transparent IR window electrodes [4], effective diffusion barriers for semiconductor applications [5] and as hard protective metallurgical coatings. It was also reported that such materials can promote *in vivo* formation of bone-like materials [6].

The incorporation of nitrogen into TiO_2 leads to at least two types of coatings: namely N-doped TiO_2 for low N content, *i.e.* the oxide structure is retained (generally anatase), and titanium oxynitride TiO_xN_y for high N content, *i.e.* the structure is different from that of the parent dioxide. The structure of TiO_xN_y coatings can be amorphous since nitrogen is known to act as a crystallization inhibitor [7] or cubic since a ternary solid solution exists between the TiN and TiO fcc phases (see Section 3.1). Starting from TiO_2 the increase of incorporated nitrogen changes the functional properties, *e.g.* refractive index and electrical conductivity as well as the mechanical properties such as hardness, elastic modulus and internal stresses of the base oxide films since metal-nitrogen bonds are less polar than the substituted metal-oxygen bonds. For instance, N-doped TiO_2 exhibits photocatalytic activity in the visible light [8,9] that is insignificant for TiO_2. On the other hand, the hardness of anatase is typically 8 GPa [10] while it increases for instance to 16.5 GPa for TiO_xN_y PVD coatings [11].

Various deposition techniques were used to produce such N-doped TiO_2 thin films such as d.c. magnetron sputtering [7,12], pulsed laser deposition [13], ion assisted electron beam evaporation [14], plasma surface treatment [15], dip coating [16], calcination of Ti compounds with N organic source [17] and metal organic chemical vapor deposition (MOCVD) [9,18,19]. Ternary TiO_xN_y hard metallurgical coatings were deposited by arc ion plating [20], d.c. reactive magnetron sputtering using a Ti target in either an $Ar/N_2/O_2$ [7,21,22] or $Ar/N_2/H_2O$ gas mixture [11,19]. The reactive sputtering process was found to be improved by pulsing the O_2 flow rate [23]. Titanium oxynitride films were prepared also by RF PECVD (plasma enhanced chemical vapor deposition) [24] and low pressure MOCVD [19,25,26]. An overview of the literature reveals few studies on TiO_xN_y coatings grown by CVD compared to PVD processes.

* Corresponding author.
E-mail address: francis.maury@ensiacet.fr (F. Maury).

doi:10.1016/j.surfcoat.2010.08.112

Amorphous TiO_xN_y coatings containing more than 23 at % N were deposited below 823 K using titanium tetra-*iso*-propoxide and NH_3 in a low pressure CVD reactor [25]. This contrasts with another claim saying that NH_3 is not effective below 823 K because the films exhibited the TiO_2 structure [26]. Possibly, this discrepancy is due to competitive mechanisms between the nitrogen incorporation, *i.e.* the growth of nitride or oxynitride, and oxidation of the nitride component, *i.e.* nitrogen release from the coating. This assumption is supported by the fact that we have observed using an original *in situ* diagnostic technique the N release from TiO_xN_y coatings for temperatures higher than 723 K in an oxidizing atmosphere [27]. Consequently, depending of the growth conditions, one of these mechanisms would be dominant and it could change rapidly. Taking into account this hypothesis, we deduce that the incorporation of nitrogen is more effective when the deposition temperature is low. This can be achieved using a nitrogen source less stable than NH_3.

Although MOCVD processes largely operate under a reduced pressure, there is also an interest to develop atmospheric pressure processes for industrial applications because no vacuum system is required and they exhibit a generally good capability for large-scale production. Coatings with a good homogeneity and a good control of the composition and microstructure can be deposited with a high growth rate. Such a process is particularly well adapted to the continuous deposition in a tunnel furnace, for instance on a flat steel scroll or on a conveyor belt set-up.

This paper deals with the deposition of TiO_xN_y coatings by atmospheric pressure MOCVD using titanium(IV) tetra-*iso*-propoxide (TTIP) and hydrazine (N_2H_4) as the N source on various substrates. The originality of this work is the use of hydrazine instead of ammonia which allows a lower deposition temperature. This new process has been developed with the goal to be applied later in a continuous deposition reactor. The configuration of the present laboratory scale reactor takes this into account. The main goal of this paper is to present the process and to describe the main features of the coatings in relation to the growth conditions. Special attention has been paid to identify the conditions leading to the growth of TiO_xN_y films and first results on mechanical properties of these hard coatings are presented.

2. Experimental

The cold-wall, vertical CVD quartz reactor, 5 cm in diameter, used for the deposition of the coatings was described elsewhere [28]. The substrates were placed on a stainless steel sample holder (3.2 cm in diameter) heated by HF induction. The substrate temperature was measured using a thermocouple inserted in the sample holder. The gas streams were monitored using mass flow controllers. Two bubblers were used for the vaporization of TTIP and hydrazine. The TTIP mole fraction was determined using a procedure previously reported [29]. The hydrazine vapor pressure was given by the relation [30]:

$$\log P(torr) = 7.8068 - 1680.74 / [T(K) - 45.41] \quad (1)$$

The N-N bond strength in hydrazine is of the same order of magnitude as for the N-H bond strength, 277 kJ/mol [31] and 337 kJ/mol [32], respectively, which is much lower than the N-H bond strength in NH_3 (450 kJ/mol) [31]. This difference in bond strength accounts for the lower thermal stability and higher reactivity of N_2H_4 compared to NH_3. As a result it can be used as the N source in MOCVD for a low deposition temperature of various nitrides as CrN [33].

The typical MOCVD conditions used for the growth of TiO_xN_y coatings are reported in Table 1. The structure of the films was determined by X-ray diffraction (XRD) using a glancing angle with an incidence of 2° (Seifert XRD 3000TT diffractometer; Cu Kα radiation). A scanning electron microscope (SEM) was used to observe the surface morphology and to measure the film thickness on cross sections (LEO-435VP microscope). The film composition was analyzed by electron probe micro-analysis (EPMA) employing a CAMECA SX-50 apparatus, secondary ion mass spectrometry (SIMS) using a CAMECA IMS 4F6 analyzer (Cs^+ bombardment) and X-ray photoelectron spectroscopy (XPS) using a VG ESCALAB MKII spectrophotometer equipped with an Mg Kα source. Adhesion of the coatings on stainless steel substrates was characterized using a scratch tester (Revetest, CSM Instrument) with a Rockwell indenter (R = 200 μm). The coatings were scratched under a normal loading rate of 10 N/min and a scratching rate of 1.29 mm/min. The hardness and elastic modulus were determined using a Berkovich nanoindenter (NanoIndenter™ II) using indentation loads in the range of 0.5-2.5 mN depending of the film thickness so that the indentation depth is less than 10% of the thickness. Tribology tests were performed at room temperature using a pin-on-disk CSEM tribometer. An alumina ball of 6 mm in diameter was used. A load of 1 N and a sliding speed of $5*10^{-2}$ m/s were applied to the samples for typically 3000 laps. Stainless steel plates (AISI 304 L), cold-rolled low carbon steel (FeP06, DIN-EN 10130), soda lime glass and Si(100) wafers were used as substrates.

Table 1
MOCVD conditions used for the growth of Ti-O-N films (explored conditions) and specific conditions for amorphous and dense TiO_xN_y coatings.

Parameters	Ti-O-N (explored conditions)	TiO_xN_y (dense coatings)
Growth temperature (K)	573 - 773	673
Total pressure (Pa)	10^5	10^5
Total gas flow rate including N_2 for dilution (sccm)	5500	5500
N_2 carrier gas flow rate for TTIP (sccm)	500 - 1250	500
N_2 carrier gas flow rate for N_2H_4 (sccm)	0 - 2000	247
N_2H_4 bubbler temperature (K)	298 - 333	313
TTIP bubbler temperature (K)	333 - 368	338
TTIP mole fraction	10^{-4} - $2.5 \cdot 10^{-3}$	10^{-4}
N_2H_4/TTIP ratio	0 - 50	20
Substrates	AISI 304 stainless steel; low C steel (FP06); Si(100); glass	AISI 304 stainless steel; low C steel (FP06); Si(100); glass
Deposition time (min)	2 - 50	15

3. Results and discussion

3.1. Composition of the Ti-O-N coatings

Two key parameters influence the growth of oxynitride coatings: (i) the deposition temperature and (ii) the N_2H_4/TTIP mole ratio R. Fig. 1 shows the variation of the N and O content in Ti-O-N films grown at 673 K with the increase of the N_2H_4/TTIP mole ratio. A good agreement was found between EPMA and XPS analyses. Three composition ranges are clearly observed corresponding to three types of coatings: (i) for R<10, N-doped TiO_2 films with N content below the detection limit of EPMA and XPS, (ii) for R>20, TiO_xN_y coatings with the constant composition $TiO_{1.5}N_{0.5}$ (*i.e.* 17 at.% N), and (iii) for 10<R<20, an intermediate range where the N content increases with the N_2H_4 partial pressure (and consequently the O content decreases) and where we assume either a continuous increase of N in a ternary solid solution or a mixture of both phases with an increase of the $TiO_{1.5}N_{0.5}$ component.

The TiO_xN_y coatings grown at a low temperature (≤673 K) and using R≥20 contain a relatively high amount of nitrogen (*ca* 17 at.% N). Increasing the temperature at 723 K, the N content decreases rapidly (not shown) to the detection limit of XPS (<0.1 at %). This is in

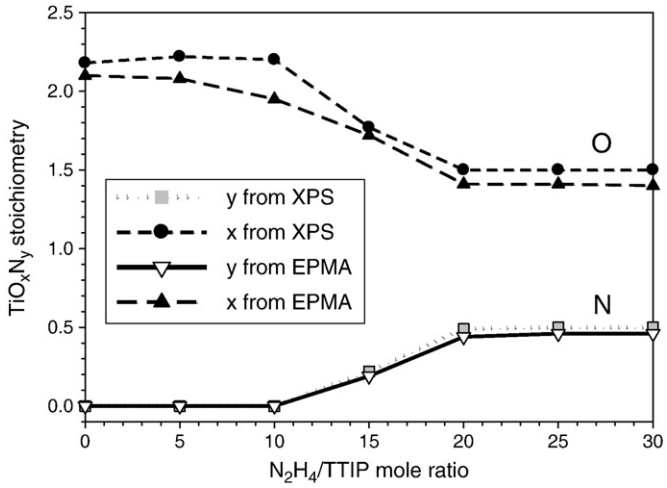

Fig. 1. Influence of the N_2H_4/TTIP mole fraction ratios of the input reactive gas phase on the oxygen (x) and nitrogen (y) stoichiometry of TiO_xN_y films grown at 673 K. The data were determined both by EPMA and XPS.

agreement with the highest stability of TiO_2 compared to TiN and titanium oxynitrides as supported for instance by the heat of formation at 1500 K of TiO_2 rutile ($\Delta Hf0 = -939$ kJ/mol), TiN (- 336 kJ/mol) and TiO_xN_y (- 358 to - 487 kJ/mol depending on the composition) [34]. This result also supports the hypothesis formulated in the Introduction stating that a competition mechanism may exist during the growth of TiO_xN_y between the nitrogen incorporation and the nitrogen release due to oxidation.

Fig. 2 shows SIMS concentration depth profiles of a thin TiO_xN_y coating (40 nm thick) grown on FP06 steel at 653 K using R = 25. The flat profiles of Ti, O and N confirm the uniform distribution of these elements through the thickness of the film. Due to the high sensitivity of SIMS analyses traces of carbon and hydrogen which could be due to incomplete decomposition of TTIP are detected. The C content is certainly very low since the signal intensity is of the same order of magnitude than in the FP06 steel substrate (*ca* 0.02 wt.% C). Due to the high sensitivity of SIMS analyses, this technique has been used to give an overview of the influence of the deposition temperature on the film

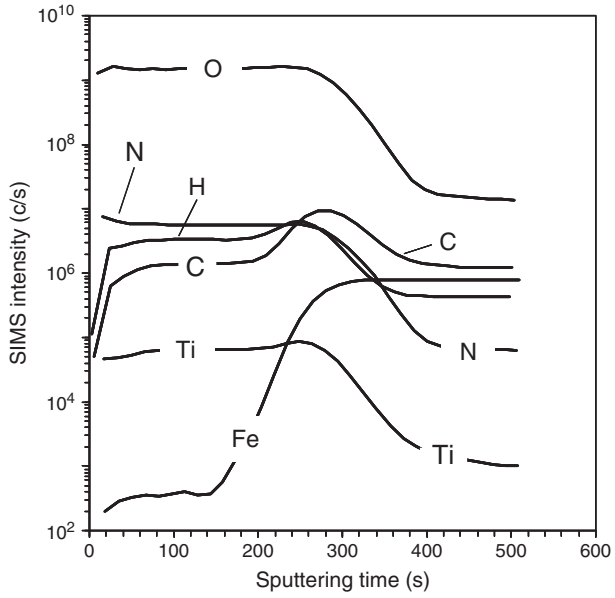

Fig. 2. SIMS depth concentration profiles of a TiO_xN_y coating 40 nm thick grown on the FP06 steel substrate at 653 K using a TTIP mole fraction of 10^{-4} and a N_2H_4/TTIP mole ratio of 25.

composition. Fig. 3 shows SIMS relative intensities of the metalloid elements (ratios N/Si, C/Si and H/Si) of Ti-O-N coatings grown on Si (100) as a function of the growth temperature using R = 15. The SIMS intensities were measured after 2 min of sputtering (*ca* 30 nm in depth). Significant composition variations are observed for N and C. The highest N content is obtained in the low temperature range 573-673 K and it rapidly decreases by increasing the temperature. The lowest C incorporation is obtained for the temperature range 623-673 K which corresponds to the formation of dense amorphous TiO_xN_y coatings as shown below. For T<623 K, a higher C contamination is found likely due to insufficient decomposition of TTIP resulting in an incorporation of organic species into the film. For T>673 K, the N incorporation is very low (<1 at %), crystallization of anatase occurs and due to the porous structure of these N-doped TiO_2 films (as we will see below) the C contamination increases again due to adsorption of atmospheric contaminants.

XPS spectroscopy was used to analyze the composition and the local bonding of the nitrogen atoms in these films. The binding energies were referred to the C 1s peak of hydrocarbon contamination fixed at 284.6 eV. Fig. 4a shows the Ti 2p spectra of films grown at 673 K for R increasing from 1.1 to 20. The spectrum of N-doped TiO_2 anatase sample (R = 1.1) shows two bands centered at 458.6 and 464.4 eV, respectively assigned to Ti^{4+} $2p_{3/2}$ and Ti^{4+} $2p_{1/2}$. This indicates that titanium in N-doped TiO_2 is in the form of Ti^{4+}, as expected for TiO_2. By increasing R, dense and amorphous TiO_xN_y coatings are obtained and a shift to lower binding energy is observed, which reveals the formation of Ti-N bonds. This shift is significant for R = 20, *e.g.* Ti $2p_{3/2}$ is found at 457.4 eV (shift = 1.2 eV), and it is accompanied by a broadening of the Ti 2p peaks which confirms a contribution of Ti^{3+} originating from the nitride or oxynitride component and possibly sub-oxides. Fig. 4b shows that the N 1s core level is not detected for R ≤ 10. Above this R value only one peak is found for N 1s at 396.4 eV, which indicates that nitrogen is incorporated in TiO_xN_y coatings in a nitride form, *i.e.* Ti-N bonds as expected for TiO_xN_y (substitutional N).

At a very high temperature (1923 K), the solubility of N in TiO_2 is very low while it is highly soluble in titanium sub-oxides. For instance a large oxynitride solid solution exists between TiO and TiN [35]. Obviously the deposition temperature in the present work is significantly lower but if we assume the same trend, by increasing the N_2H_4/TTIP mole ratio, the growth of TiO_2 competes locally with that of TiO_x and possibly TiN at the surface of the growing film due to

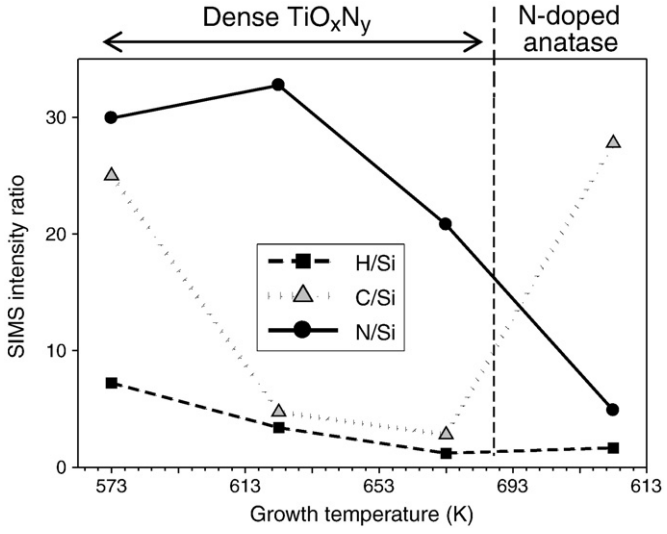

Fig. 3. Influence of the deposition temperature on the relative composition of the metalloid elements in Ti-O-N coatings grown on the Si(100) substrate. The relative content of N, C, and H was estimated from the SIMS intensity ratios normalized to the signal of the Si substrate. An N_2H_4/TTIP mole ratio of 15 was used for the deposition.

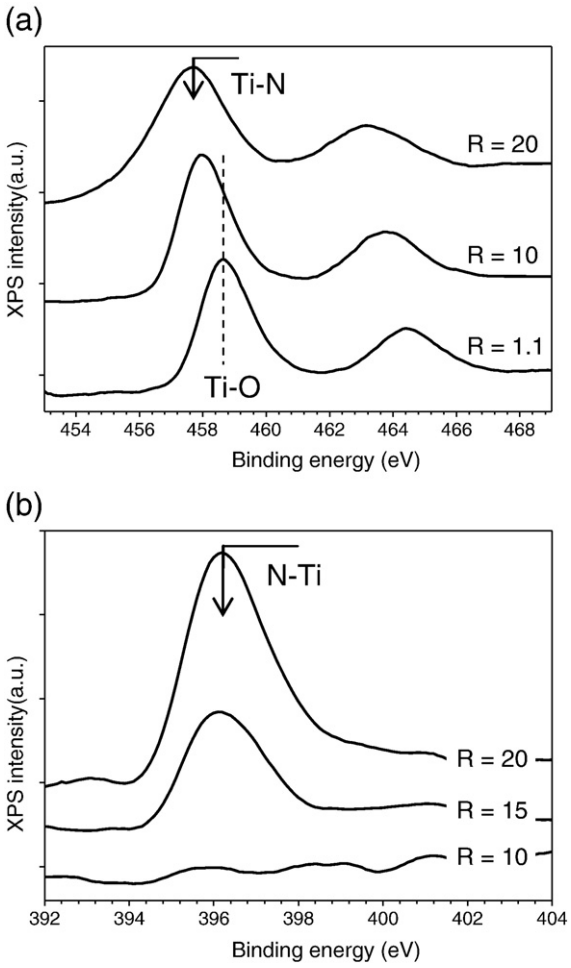

Fig. 4. High resolution XPS spectra of Ti-O-N films grown on Si(100) at 673 K using different N_2H_4/TTIP mole ratios R from 1.1 to 20: (a) Ti $2p_{3/2}$ and Ti $2p_{1/2}$ and (b) N 1s spectral range.

the presence of hydrogen and nitrogen resulting from the decomposition of N_2H_4. As a result, TiO_2 can be partially reduced into suboxides and N becomes soluble to form TiO_xN_y coatings.

3.2. Morphology and appearance of the Ti-O-N coatings

The films containing a low amount of nitrogen (N-doped TiO_2) are transparent in the visible range and they exhibit various bright colors depending on their thickness (interferential colors) as observed for undoped TiO_2 films [28]. Typically, for thicknesses higher than 500 nm, by increasing progressively the N_2H_4/TTIP mole ratio the transparency of the films in the visible range decreases. They exhibit a green color for low R values and become dark-green with an increasing opacity, then metallic in appearance by increasing R. We also observed that the film thickness uniformity across the substrate is better for this type of coating than for TiO_2 films.

The Fig. 5a to c shows the surface topography of Ti-O-N films deposited on stainless steel at 673 K using different N_2H_4/TTIP mole ratios. For the low value of R ($\leq$5.5) a granular-like surface morphology is observed (Fig. 5a and b). However cross sections give evidence for a columnar growth as observed for undoped TiO_2 [28] revealing that the granular-like structure observed on the surface is the domes of the columns (Fig. 5d and e). Separation between columns leads to a fairly large open porosity. By increasing R from approximately 5 to 15, a compact and thin underlayer is formed at the interface to the substrate from which elongated crystallites with angular domes grow to form the columns (Fig. 5d and e). This heterogeneous structure suggests the presence of two phases. The thickness of this underlayer increases with R and the elongated crystallites disappear completely for R$\geq$20 leading to very dense coatings (Fig. 5f). They have a very smooth surface morphology with an RMS roughness measured using an optical profilometer of 20 nm for a film thickness of 1 μm (Fig. 5c and f).

The temperature also influences drastically the morphology of the Ti-O-N layers. For R$\geq$20, the coatings obtained for temperatures between 573 and 673 K are very smooth and compact as in Fig. 5f, while for temperatures higher than 693 K they exhibit a columnar morphology as for instance in Fig. 5d. These critical temperatures are strongly related to the N content as shown in the Fig. 3.

3.3. Structure of the Ti-O-N coatings

The oxynitride coatings grown at 673 K are constituted of anatase for low N_2H_4/TTIP ratios (R$\leq$5.5) as shown in Fig. 6. Traces of rutile are also observed for films grown on stainless steel but not on glass and Si substrates. Increasing R leads to a degradation of the crystallinity of the anatase phase and amorphous layers are obtained for R>10. A similar behavior is observed for films grown on glass, silicon and stainless steel substrates. No evidence for the formation of the fcc phases TiN or TiO_xN_y was found by XRD when R > 10. Nitrogen is incorporated in the oxide matrix to form a homogenous ternary compound (single phased) with the typical composition $TiO_{1.5}N_{0.5}$. Because N is not soluble in TiO_2 its acts as a crystallization inhibitor and an amorphous structure is formed. A similar behavior was previously reported for sputtered TiO_xN_y films [7]. Since the XRD pattern did not reveal the presence of crystalline phases, the substitution of O by N is supposed to occur randomly.

3.4. Growth rate of the dense and amorphous TiO_xN_y coatings

The thickness of the TiO_xN_y films increases linearly with the deposition time (not shown). This indicates a constant growth rate over several tens of minutes and permits a good reproducibility of the deposition process. The growth rate of dense and amorphous TiO_xN_y coatings in the temperature range 573-693 K and for R = 20 was found only slightly dependent on the deposition temperature with an apparent activation energy of only 6 kJ/mol (Fig. 7a). Above 693 K the kinetic regime changes due to the growth of anatase and the activation energy increases to values previously found for pure TiO_2 (*ca* 35 kJ/mol).

Likely N_2H_4 acts as a catalyst enhancing the decomposition of TTIP and the growth rate is not kinetically controlled as supported by the low activation energy found in the temperature range 573-693 K which indicates a physical limitation. Usually, in CVD processes, when the growth rate is limited by the mass transport it increases linearly with the partial pressure of the reactant. Fig. 7b shows a quasi-linear dependence of the growth rate with the TTIP mole fraction in the range 0.02-0.30% indicating that the process is controlled by the mass transport of TTIP. The use of these high TTIP flow rates allows reaching a growth rate as high as *ca* 14 μm/h which is consistent with a surface treatment to scrolling. Possibly a change in the kinetics mechanism occurs for the lowest TTIP mole fractions ($<10^{-4}$) that corresponds to a high dilution of the reactive gas phase. These particular conditions have not been investigated because they lead to very low growth rates. Furthermore a complete kinetics study of this process was not the objective at this stage.

Frequently, in CVD, when the growth rate has to be optimized this can be achieved by increasing the deposition temperature. However for this particular process, Fig. 7a showed that this process was only very weakly activated by the temperature. Nevertheless these compact and amorphous TiO_xN_y coatings can be obtained at temperatures higher than 673 K by using N_2H_4/TTIP mole ratios higher than 20. A deposition diagram showing the existence area of

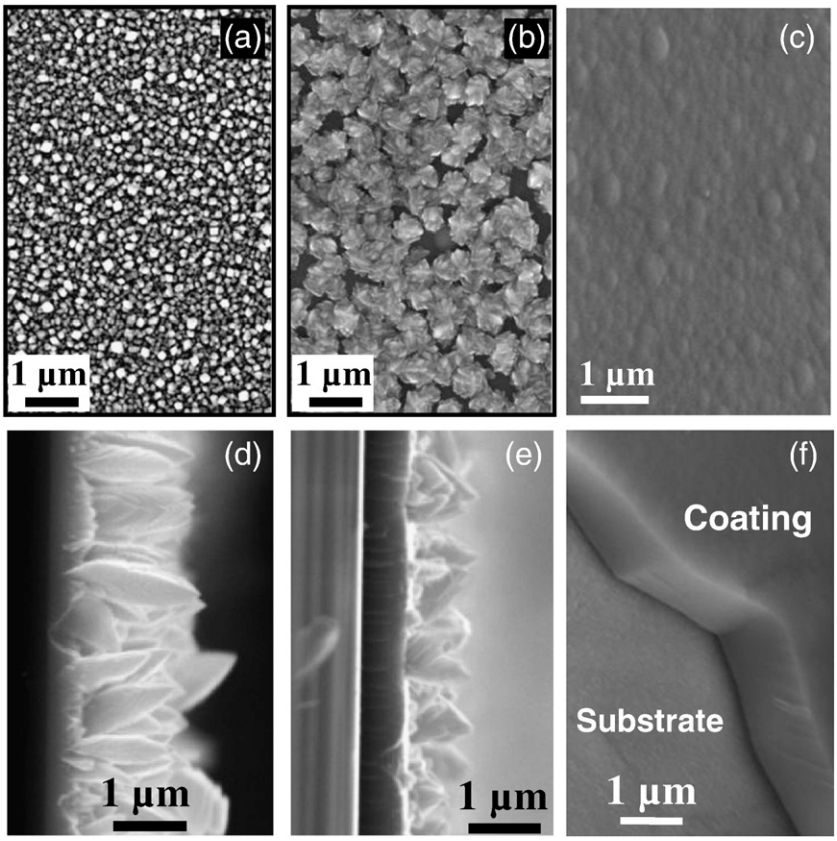

Fig. 5. SEM micrographs of Ti-O-N films showing the surface topography and cross sections. Coatings were grown under atmospheric pressure on stainless steel substrates at 673 K using a TTIP mole fraction of 10^{-4} and various N_2H_4/TTIP mole ratios R: (a) R = 1.1; (b) R = 5.5; (c) R = 20; (d) R = 5.5; (e) R = 10 and (f) R = 20. The micrographs c and f correspond to a dense and amorphous $TiO_{1.5}N_{0.5}$ coating.

dense and amorphous TiO_xN_y coatings as a function of temperature and TTIP mole fraction is presented in Fig. 8 (this diagram is focused on this transition). Dense and amorphous TiO_xN_y (~17 at % N) coatings are grown at low temperatures (≤673 K) using low values of TTIP mole fractions (R is maintained at 20). In this low temperature range the existence area of TiO_xN_y coating is large and the TTIP mole fraction can be increased for instance to increase the growth rate. Thus by increasing the TTIP mole fraction (10<R<15), the films are still dense and amorphous but the N content decreases. For R < 10, the film exhibits a composite structure constituted of anatase and the amorphous phase as shown typically in the Fig. 5d and e. The amount of crystalline anatase decreases by increasing R. At a high temperature, the growth of N-doped TiO_2 (anatase) is preferred which confirms that the deposition of TiO_xN_y coating by CVD requires low temperatures.

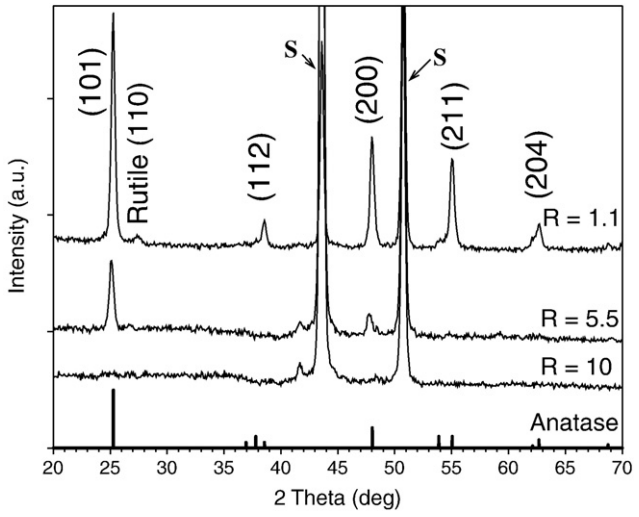

Fig. 6. Glancing angle XRD spectra (incidence angle 2 deg) of Ti-O-N coatings grown at 673 K on stainless steel using a TTIP mole fraction of 10^{-4} and N_2H_4/TTIP mole ratios R equals to 1.1, 5.5 and 10. The peaks labeled S originate from the substrate. The JCPDS card of anatase (#84-1285) is given at the bottom.

3.5. Mechanical properties of dense and amorphous TiO_xN_y coatings

The main interest of the N-doped TiO_2 thin films is for their functional optical and photocatalytic properties [9]. Consequently their mechanical properties were not investigated and we focused on the dense and amorphous TiO_xN_y coatings.

Hardness measured by nanoindentation increases with the nitrogen content to reach 19.5 (±4.5) GPa for a $TiO_{1.5}N_{0.5}$ coating with a thickness of 1 µm. This is almost three times higher than that of the 304 L stainless steel substrate (6.9 GPa). This is also significantly higher than the 8 GPa reported for anatase films [10]. This $TiO_{1.5}N_{0.5}$ CVD coating (1 µm thick) is as hard if not more than as those (400 nm thick) deposited by d.c. reactive sputtering (16.5 GPa) [11]. These authors have also reported a decrease of the hardness when the nitrogen content decreases. The Young's modulus of the CVD film (250 ± 45 GPa) is close to the value of the steel substrate (222 ± 15 GPa), indicating a good adherence of the film. The relatively high value of the H^3/E^2 ratio (0.12) indicates a good resistance of the

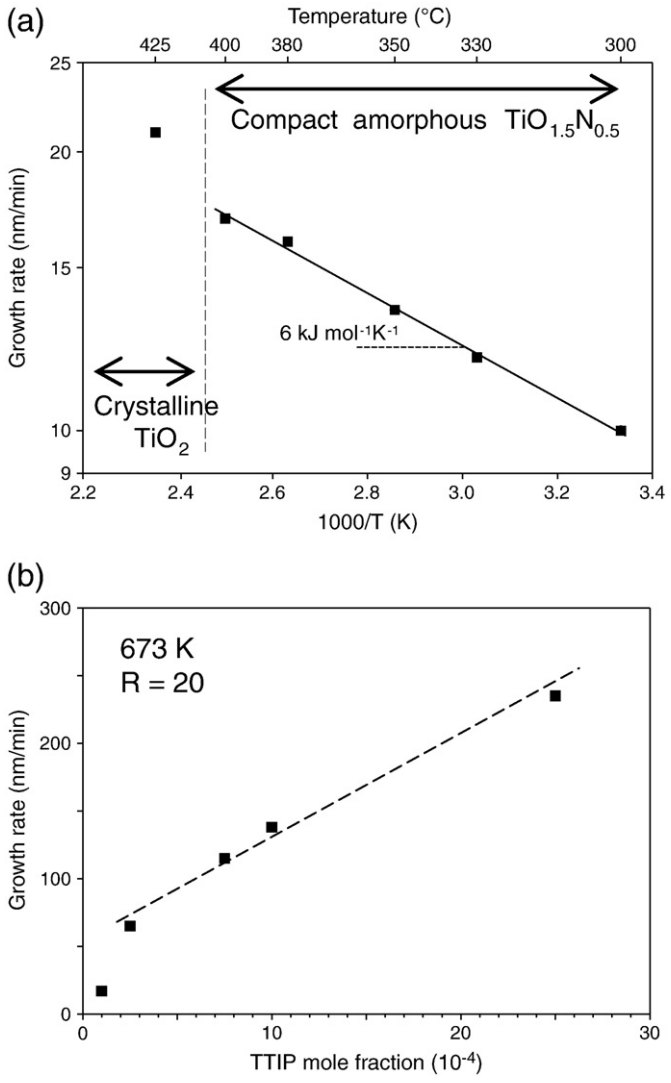

Fig. 7. Dependence of the growth rate of TiO_xN_y dense coatings grown on Si(100) as a function of (a) the deposition temperature (R = 20; TTIP mole fraction = 10^{-4}) and (b) the TTIP mole fraction (R = 20; 673 K).

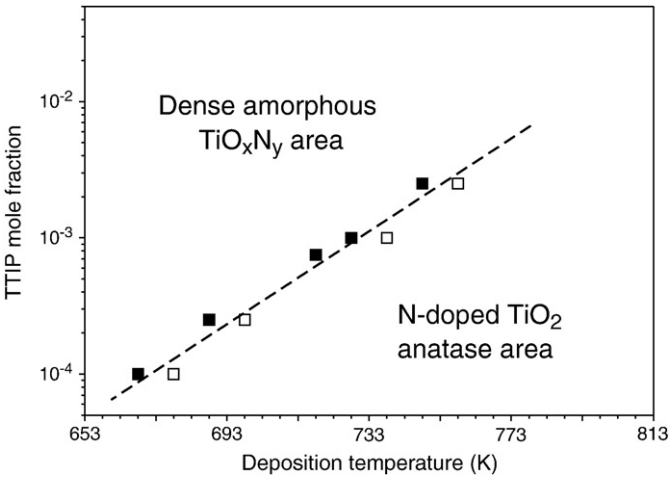

Fig. 8. Influence of deposition temperature and the TTIP mole fraction on the transition between the areas of existence of the two types of coatings obtained on stainless steel using an N_2H_4/TTIP ratio of 20: dense and amorphous TiO_xN_y coatings above the straight line and N-doped TiO_2 anatase films below the line.

coating to plastic deformation. The Young's modulus of these CVD coatings is similar to that of sputtered TiO_xN_y coatings (240 MPa) [11] which confirms that both coatings have comparable behaviors.

A compressive residual stress of 850 MPa was determined for a $TiO_{1.5}N_{0.5}$ coating using the Stoney equation from the change in curvature before and after the deposition on a thin stainless steel coupon (720 μm thick) [36]. This compressive residual stress could have a beneficial effect on the fatigue life and stress corrosion because it delays crack initiation and propagation. Compressive stresses around 400 MPa were reported for sputtered TiO_xN_y coatings grown at room temperature with comparable composition [22]. The high value of the residual stress of our CVD coating is likely due to the difference in the thermal expansion coefficient of the film and the substrate. However the N content of the film and the growth conditions strongly influence the compressive stresses of sputtered TiO_xN_y coatings since values as high as 5 GPa were measured [20].

Adhesion of a $TiO_{1.5}N_{0.5}$ coating (2.5 μm thick) on stainless steel has been characterized using a scratch tester. Microscopy observations of the track showed no damage for loads lower than 3.2 N. The first cracks in the track occur for a critical load higher than 3.2 N and are a characteristic of a cohesive failure. Increasing the load, spalling and buckling failure modes with regular chippings on each side of the track were observed around 14 N as a result of compressive stress field preceding the moving stylus. This chipping mode mechanism is a characteristic of hard coatings. This test confirms the good adhesion of the coating on stainless steel.

Fig. 9 shows the variation of the friction coefficient for a $TiO_{1.5}N_{0.5}$ coating (2.5 μm thick) on stainless steel. Measurement on the bare substrate was stopped after only 1000 laps because of the highly noisy signal due to the poor friction coefficient of the stainless steel. For the $TiO_{1.5}N_{0.5}$ coating, a steady-state regime is reached after only a few meters of sliding and the friction coefficient reaches 0.18. After approximately 1100 laps (*ca* 60 m) the formation of wear debris increases slightly the friction coefficient to approximately 0.21. The wear tracks were analyzed by optical profilometry (insert of Fig. 9) and the wear rates of the coating were calculated according to [37]. The calculated value is $8.1*10^{-7}$ mm^3 N^{-1} m^{-1}, while the wear rate of the stainless steel substrate is $8.6*10^{-4}$ mm^3 N^{-1} m^{-1}, *i.e.* 3 orders of magnitude higher.

4. Conclusions

Titanium oxynitride thin films have been deposited by atmospheric pressure MOCVD using TTIP and N_2H_4 as reactive gases. This is an original process for which the deposition temperature and the mole fraction ratio N_2H_4/TTIP are the key parameters. For a given

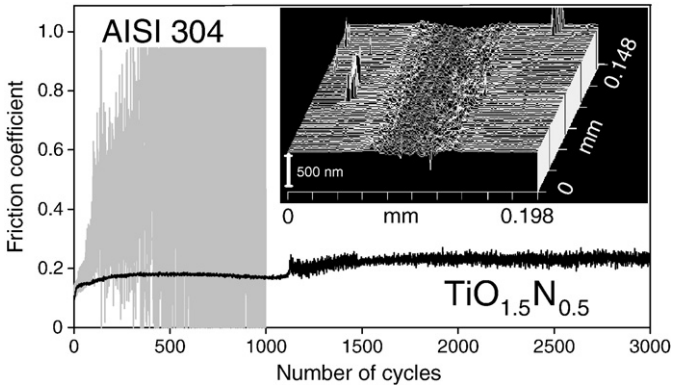

Fig. 9. Variation of the friction coefficient of a hard $TiO_{1.5}N_{0.5}$ coating 2.5 μm thick (black curve) and stainless steel AISI 304 (grey curve). The insert shows the optical profilometry image of the wear track of the $TiO_{1.5}N_{0.5}$ coating grown on the stainless steel disk after the tribology test. Growth conditions of the sample: 673 K; R = 20; TTIP mole fraction = 10^{-4}.

temperature, typically 673 K, the N content of the film is controlled by the N_2H_4 mole fraction. The variation of the N content in the films significantly changes the structure and, consequently, the functional and mechanical properties. When low amounts of N are incorporated the films are identified as N-doped TiO_2 anatase layers which exhibit the functional properties expected for this wide band gap semiconductor, for instance photocatalytic activity in the visible range [9]. When high N_2H_4 partial pressures are used the resulting films contain approximately 17 at.% N; they become amorphous, very dense and they exhibit a smooth surface morphology. These $TiO_{1.5}N_{0.5}$ coatings are typically deposited at 673 K using a N_2H_4/TTIP ratio of 20 with a growth rate as high as 14 μm/h. Many works have been reported on PVD of comparable titanium oxynitride coatings, especially by d.c. reactive sputtering [7,11,19,21–23]. Comparatively there is little research on CVD and this is the first process operating under atmospheric pressure for the growth of $TiO_{1.5}N_{0.5}$ coatings. It was demonstrated that low temperatures are required which is achieved using hydrazine as the N source. First studies on the mechanical properties of these coatings confirm their potential as protective metallurgical coatings. They exhibit a high hardness (19.5 GPa), a compressive residual stress of 850 MPa, a good adhesion on stainless steel, a low friction coefficient (0.2) and a good wear resistance.

References

[1] J. Bartella, J. Schroeder, K. Witting, Appl. Surf. Sci. 179 (2001) 181.
[2] Y. Zheng, K. Kikuchi, M. Yamasaki, K. Sonoi, K. Uehara, Appl. Opt. 36 (1997) 6335.
[3] Y. Saito, M. Hirata, H. Tada, M. Hyodo, Appl. Phys. Lett. 63 (1993) 1319.
[4] C.F. Wan, F.C. Sulzbach, J.D. Luttmer, J. Vac. Sci. Technol., B 10 (1992) 1658.
[5] Y.H. Ku, S.K. Lee, D.L. Kwong, Thin Solid Films 172 (1989) 1.
[6] S. Piscanec, L. Colombi Ciacchi, E. Vesselli, G. Comelli, O. Sbaizero, S. Meriani, A. De Vita, Acta Mater. 52 (2004) 1237.
[7] S.H. Mohamed, O. Kappertz, T. Niemeier, R. Drese, M.M. Wakkad, M. Wuttig, Thin Solid Films 468 (2004) 48.
[8] R. Asahi, T. Morikawa, T. Ohwaki, K. Aoki, Y. Taga, Science 293 (2001) 269.
[9] F.-D. Duminica, F. Maury, R. Hausbrand, Surf. Coat. Technol. 201 (2007) 9349.
[10] O. Zywitzki, T. Modes, H. Sahm, P. Frach, K. Goedicke, D. Glöß, Surf. Coat. Technol. 180–181 (2004) 538.
[11] J.M. Chappe, J. Gavoille, N. Martin, J. Lintymer, J. Takadoum, J. Mater. Sci. 41 (2006) 5639.
[12] G.R. Torres, T. Lindgren, J. Lu, C.-G. Granqvist, S.-E. Lindquist, J. Phys. Chem. B 108 (2004) 5995.
[13] Y. Suda, H. Kawasaki, T. Ueda, T. Ohshima, Thin Solid Films 453–454 (2004) 162.
[14] M.-C. Yang, T.-S. Yang, M.-S. Wong, Thin Solid Films 469–470 (2004) 1.
[15] L. Miao, S. Tanemura, H. Watanabe, Y. Mori, K. Kaneko, S. Toh, J. Cryst. Growth 260 (2004) 118.
[16] M. Miyauchi, A. Ikezawa, H. Tobimatsu, H. Irie, K. Hashimoto, Phys. Chem. Chem. Phys. 6 (2004) 865.
[17] T. Ihara, M. Miyoshi, Y. Iriyama, O. Matsumoto, S. Sugihara, Appl. Catal., B: Environmental 42 (2003) 403.
[18] C. Sarantopoulos, A.N. Gleizes, F. Maury, Thin Solid Films 518 (2009) 1299.
[19] J. Guillot, J.-M. Chappe, O. Heintz, N. Martin, L. Imhoff, J Takadoum, Acta Mater. 54 (2006) 3067.
[20] Y. Makino, M. Nose, T. Tanaka, M. Misawa, A. Tanimoto, T. Nakai, K. Kato, Surf. Coat. Technol. 98 (1998) 934.
[21] N. Martin, O. Banakh, A.M.E. Santo, S. Spinger, R. Sanjines, J. Takadoum, F. Levy, Appl. Surf. Sci. 185 (2001) 123.
[22] S. Venkataraj, D. Severin, S.H. Mohamed, J. Ngaruiya, O. Kappertz, M. Wuttig, Thin Solid Films 502 (2006) 228.
[23] N. Martin, J. Lintymer, J. Gavoille, J.M. Chappe, Surf. Coat. Technol. 201 (2007) 7720.
[24] C.K. Jung, I.S. Bae, Y.H. Song, S.J. Cho, J.H. Boo, Solid State Phenom. 111 (2006) 151.
[25] F. Fabreguette, L. Imhoff, J. Guillot, B. Domenichini, M.C. Marco de Lucas, P. Sibillota, S. Bourgeois, M. Sacilottia, Surf. Coat. Technol. 125 (2000) 396.
[26] S.K. Pradhan, P.J. Reucroft, J. Cryst. Growth 250 (2003) 588.
[27] F.-D. Duminica, F. Maury, Surf. Coat. Technol. 202 (2008) 2423.
[28] F.-D. Duminica, F. Maury, F. Senocq, Surf. Coat. Technol. 188–189 (2004) 255.
[29] F. Maury, F.-D. Duminica, F. Senocq, Chem. Vap. Deposition 13 (2007) 638.
[30] D.W. Scott, G.D. Oliver, M.E. Gross, W.N. Hubbard, H.M. Huffman, J. Am. Chem. Soc. 71 (1949) 2293.
[31] David R. Lide (Ed.), CRC Handbook of Chemistry and Physics; 90th Edition, Internet Version, 2010, p. 9.
[32] B. Ruscic, J. Berkowitz, J. Chem. Phys. 95 (1991) 4378.
[33] F. Schuster, F. Maury, J.F. Nowak, C. Bernard, Surf. Coat. Technol. 46 (1991) 275.
[34] B. Granier, J.P. Coutures, Comptes Rendus Acad. Sci. Paris, série C 290 (1980) 275.
[35] B. Granier, R. Renard, J.P. Coutures, Rev. Int. Hautes Temp. Refract. 17 (1980) 235.
[36] G.G. Stoney, Proc. R. Soc. London, Ser. A 82 (1909) 172.
[37] K. Holmberg, A. Matthews, in: D. Dowson (Ed.), Coating Tribology, Tribology Series, 28, Elsevier, Amsterdam, 1994.